Side Lobe Level Reduction in Horn Antennas using Graphene

Hadi Balegh
Department of Electrical and Computer Engineering
Tarbiat Modares University
Tehran, Iran, P.O.Box 14115-111
Email: H.balegh@modares.ac.ir

Bijan Abbasi Arand
Department of Electrical and Computer Engineering
Tarbiat Modares University
Tehran, Iran, P.O.Box 14115-111
Email: Abbasi@modares.ac.ir

Leila Yousefi
School of Electrical and Computer Engineering
University of Tehran
Tehran, Iran
Email: Lyousefi@ut.ac.ir

***Abstract*—This paper proposes a novel method to suppress the side-lobe level of pyramidal horn antennas using graphene sheets. Using numerical full wave simulation, it is shown that loading graphene sheet inside the horn antenna leads to a tapered aperture field distribution, resulting in side-lobe level reduction. Graphene length and surface impedance are optimized with the purpose of achieving a low side-lobe level of $-31dB$ while keeping the antenna gain as high as possible. In comparison to traditional metallic horn antennas (Metal-based horn), hybrid graphene-metal horn (Graphene-based horn) presents a truly smooth radiation pattern and improves the side-lobe by $17.6dB$. In essence, graphene sheet acts as a high impedance surface (HIS) and hinders electromagnetic energy from reaching to horn aperture edges, so diffraction phenomenon is drastically diminished. Consequently, ripples and minor lobes are excluded from the radiation pattern of the proposed antenna .**

***Keywords*—graphene; horn antennas; side-lobe; radiation pattern; diffraction.**

I. Introduction

Graphene with a gapless and linear electronic band-structure has opened up new developments in currently high-tech researches. It is truly a monolayer of carbon atoms packed into a honeycomb lattice. This quasi-two-dimensional (2D) is the thinnest and strongest material has been discovered up to now. Furthermore, Furthermore, its performance surpasses that of any other material as a conductor of heat and electricity. These advantages of graphene and its controllable behavior with an external bias voltage has engrossed researchers attention around the world [1]-[4]. Graphene surface conductivity, one of the important characteristics of this extraordinary material, can be tuned by an external magnetic or electrostatic bias field. Graphene flakes could be grown on copper with the appreciable size of 30 inches by chemical vapor deposition (CVD) using methane [5]-[7]. The possibility of manufacturing graphene in large sizes has provided situations for using this material at microwave and millimeter-waves frequencies. In recent years, graphene has been manipulated as an electromagnetic waveguide medium to improve passive RF components (i.e. transmission lines , filters, couplers, and interconnectors) [8]-[11].

Low side-lobe level (SLL) antennas are extensively used for applications which require high directivity such as radar systems, tracking devices and getting rid of electromagnetic interference [12]-[13]. Diffractions from horn antennas aperture edge, strongly distort their radiation pattern and cause undesired radiations [14]. For decades, distinctive methods have been suggested to control side lobe in horn antennas. Metamaterials [5]-[6], wire mediums [12], corrugated surfaces [15]-[19], non-uniform slot arrays [20], frequency selective surfaces [9] and forming the edges of aperture [21] are some of these typical methods exploited to moderate the side lobe level of horn antennas.

Aforementioned approaches have some conspicuous deficiencies like fabrication difficulties and incontrollable far-field radiation specification. Therefore, a flexible method which can reduce the side lobe level of the antenna and control it at the same time would be beneficial in designing high-gain antennas. High impedance surfaces (HIS) can decrease the side-lobe level of an antenna by suppressing surface currents [22] .

This paper suggests a new method to adjust and reduce the side-lobe level of horn antennas using graphene sheets. Here we exploit the high impedance property of graphene to suppress surface currents, and control the side lobe in horn antennas. Since the surface impedance of graphene sheet can be altered by applying an external voltage, graphene can be used as a controllable HIS for adjusting the far-field radiation pattern of microwave antennas.

The advantages of the proposed method in comparison, with previously developed approaches is its ability to control the side-lobe level of Metal-based horn antennas, and also simple fabrication.

II. Modeling of Graphene Surface Conductivity

Graphene surface conductivity which can describe electromagnetic properties of graphene is an extremely important parameter in modelling of this material. In the absence of the magnetic bias field, this surface conductivity can be defined by Kubo formula [23]. At microwave, and low terahertz frequencies, intraband contribution of graphene conductivity simply prevails over the interbnad contribution at room temperature [24]. Therefore, graphene surface conductivity at microwave frequencies can be expressed by intraband contribution, as follows [24]:

$$\sigma = \frac{e^2 k_B T}{\pi \hbar^2 (2\Gamma + j\omega)} \left[\frac{\mu_c}{K_B T} + 2 \ln \left(e^{(-\frac{\mu_c}{K_B T})} + 1 \right) \right] \quad (1)$$

where ω is the radial frequency, $-q_e$ is the charge of an electron, $\hbar$ is the reduced Planks constant, $\Gamma = 1/2\tau$ is the electron scattering rate, while τ is the electron relaxation time, T is the room temperature, K_B is the Boltzmanns constant, μ_c is graphene chemical potential. The Fermi velocity is set to $v_f = 9 \times 10^5 m/s$, temperature is $T = 300K$ and electron relaxation time is $\tau = 0.1ps$ throughout the paper.

Another important characteristic of graphene is the surface impedance which is correlated to graphene conductivity as $Z_s = 1/\sigma$. As shown in (1), graphene surface impedance can be dynamically tuned by controlling graphene chemical potential μ_c, which may be adapted by material initial doping or by applying a transverse electrical field. So, graphene chemical potential can be adjusted by an external bias voltage V_b through [25]-[26]:

$$\mid \mu_c \mid \approx \mid E_f(V_b) \mid \approx \hbar v_f \left[\pi a_0 \mid V_b - V_{Dirac} \mid \right]^{1/2} \quad (2)$$

where $a_0 = 9 \times 10^{16} m^{-2} V^{-1}$ is calculated from a single capacitor model[26], and $V_{Dirac} = 0.8V$ is the voltage offset produced by natural doping of graphene.

III. Controlling and Suppressing Side-lobes Radiations of Horn Antenna by Loding Graphene Sheets

The configuration of the proposed hybrid graphene-metal horn antenna (Graphene-based horn) is shown in Fig. 1. As shown in this figure, graphene sheets are deposited on the inner walls of the traditional pyramidal horn antenna (Metal-based horn) designed to operate at the frequency of $10GHz$. The standard X-band waveguide is used in the proposed structure, to feed the antenna. The waveguide dimensions are $a = 0.9in$

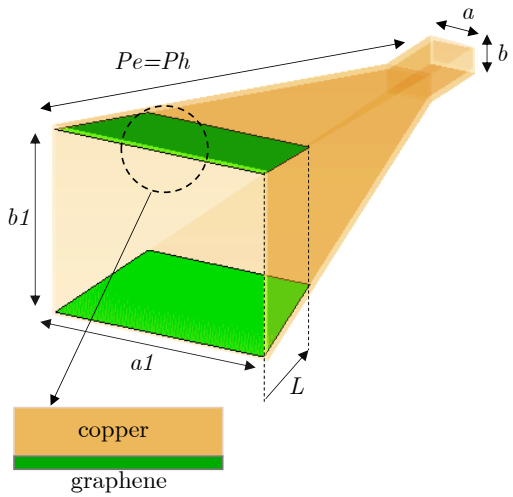

Fig. 1: The proposed horn antenna in which graphene sheets are used to suppress the sidelobes $a = 0.9in$,$b = 0.4in$, $P_e = P_h = 10.06in$, $a_1 = 4.87in$ and $b_1 = 3.62in$.

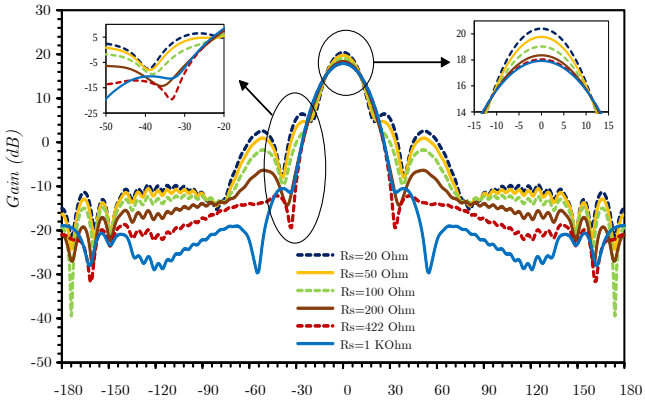

Fig. 2: The E-plane radiation pattern of Graphene-based horn for different surface resistances(R_s) of graphene. Insets illustrate the antenna side-lobe level and gain variations.

and $b = 0.4in$. The aperture sizes of the horn are $a_1 = 4.87in$ and $b_1 = 3.62in$.

Furthermore, P_e and P_h are antenna dimensions measured from the antenna phase center in $E-$ and $H-$planes, respectively. Graphene sheets are grown on upper and lower walls of the antenna by chemical vapor deposition (CVD). Their length (L) is measured from the antenna aperture, as shown in Fig. 1. We simulate the proposed structure by the frequency-domain solver of CST Microwave studio. In this paper, graphene layers are modelled as an infinitesimally thin sheets ($2D$ sheets), with the surface impedance ($Z_s = 1/\sigma = R_s + jX_s$) calculated using Kubo Formula as explained in section II.

Here, we perform a parametric study to achieve optimal values for parameters of the graphene sheets. The graphene sheets surface impedance (Z_s) and their length (L) play a decisive role in the side-lobe level (SLL), front to back ratio (F/B) and gain of the horn antenna. Varying graphene sheet length in the range of $1in \leq L \leq 11.6in$, where its surface impedance assumed to be $Z_s = 422\Omega$, the side-lobe level is reduced as the graphen length increases, but at the same time F/B is reduced too. As previously mentioned, the diffraction happens at the antenna aperture edges, so increasing graphene sheets length produce further losses without any alteration in SLL and F/B of the radiation pattern. Consequently, we choose sheets length as $L = 2.8in$ resulting in SLL equal to $\sim -31dB$ and F/B ~ 40 dB.

Another parameter which deserves some investigations is graphene surfaces impedance (Z_s). We vary the surface impedance in the range of $50\Omega \leq Z_s \leq 1K\Omega$, while graphene sheet length is considered to be $L = 2.8in$. Simulated results indicate that side-lobe level takes its lowest value at $Z_s \approx 450\Omega$ resulting in $SLL \approx -31dB$ and front to back ratio equal to $F/B \approx 40dB$. As a matter of fact, graphene sheet can act as a high impedance surface at $10GHz$. Thereby, it doesnt allow surface currents to reach antenna aperture edges. Also, graphene eliminates diffractions which causes undesired minor lobes and ripples in the antenna radiation pattern. Up to now, we have optimized graphene physical and electrical parameters in order to achieve a low side lobe radiation pattern for the horn antenna. Another important parameter is antenna gain which

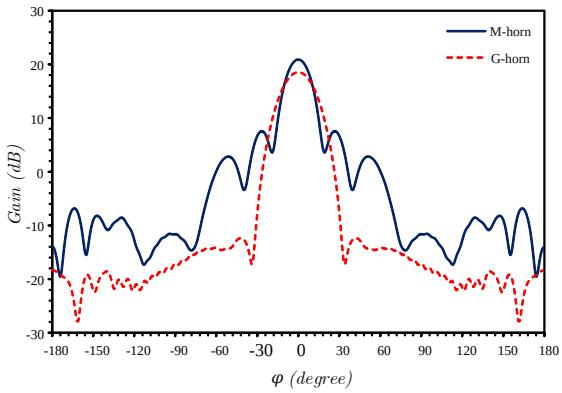

(a)

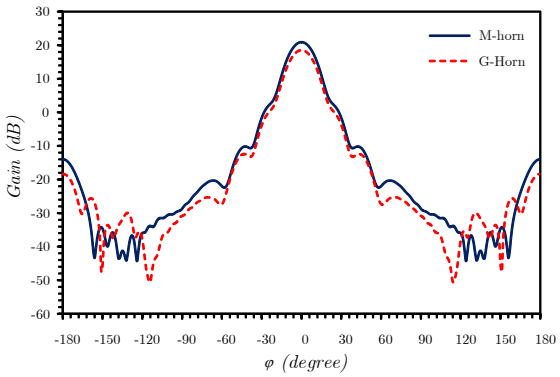

(b)

Fig. 3: Radiation pattern of the proposed Graphene-based horn antenna is comapred with that of regular metallic horn. (a) E-palne pattern,(b) H-Plane pattern.

can be affected by variation of graphene surface impedance and its length.We have shown the numerically calculated gain of the pyramidal Graphene-based horn antenna in Fig. 2. As the results of this figure shows, as the surface impedance of graphene sheet increases the gain decreases, however for the impedance $Z_s \approx 450\Omega$, the gain is acceptable and only decreases from $\sim 21dB$ to $\sim 18.5dB$. In the rest of this paper, graphene sheets length are fixed at $L = 2.8in$ for all of the presented simulations.

To have a comprehensive contemplation on simulated results of proposed structure, here, we investigate how graphene surface resistance (R_s) controls the radiation pattern, side-lobes and the main-lobe. Fig. 2 demonstrates the E-plane radiation pattern of the proposed antenna for various graphene film surface impedances. As shown in this figure, we could adapt the side-lobe level of the radiation pattern to make it suitable for different purposes. The large variation of the radiation pattern SLL with the bias voltage is the fascinating feature of the recommended method, which is depicted in the left inset of Fig. 3. Besides, the gain variation is shown in the right inset of this figure. We recognize that variation of the side-lobe level in the range of $-15dB \lesssim SLL \lesssim -31dB$, results a variable gain within the range of $18.5dB \lesssim Gain \lesssim 21dB$, where graphene surface resistance ($50\Omega \leq R_s \leq 450\Omega$) can get any feasible

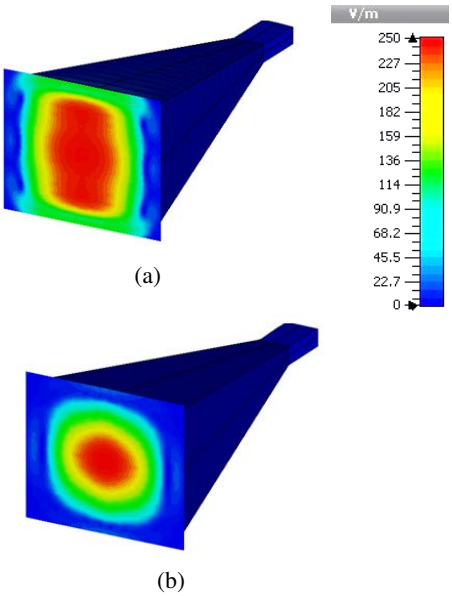

(a)

(b)

Fig. 4: Amplitude of the electric field on the antenna aperture. (a) Regular Metal-based horn,(b) Proposed Graphene-based horn.

values. In the rest of this paper, graphene surface resistance is chosen as ($R_s = 450\Omega$) to achieve the lowest possible level for the side-lobe level.

Now the proposed Graphene-based horn is compared with the regular Metal-based horn antenna which doesnt have any graphene in its structure. The $E-$ and $H-$plane radiation patterns of these two structure at the frequency of $10GHz$ have been illustrated in Fig. 3a. and Fig. 3b. In comparison to SLL of the Metal-based horn, the SLL of the proposed Graphene-based horn has been significantly decreased around $\sim 17.6dB$, according to Fig. 3a. However, Due to negligible current distribution on the side walls of the horn antenna, the H-plane radiation pattern of these two structures do not have any noticeable difference with each other .

Fig. 4. compares the E-field distribution at the aperture of the two antennas. As shown in this figure, the electric field distribution over the antenna aperture is tapered along the H-direction (x direction) and almost uniform along E-direction (y direction). The aperture distribution in the normal antenna causes a narrow beam-width and high side-lobes in the antenna E-plane radiation pattern, as shown in Fig. 3a., and also in Fig. 5a. However, as shown in Fig. 4b., the horn antenna with Graphene deposited on the inner walls, has tapered E-field over the antenna aperture. As shown in Fig. 4b., the amplitude of the electric field is tapered in E-direction. Besides, it is mostly concentrated on the central part of the antenna and drastically decreased on edges of the antenna aperture. As shown in Fig. 5b., this tapered aperture field results in radiation pattern with significantly smaller side lobes.

To investigate more about the reason behind these results, here we look at the current distribution on inner walls of these two structures. For Metal-based horn, surface currents reach to aperture edges of the antenna without any percep-

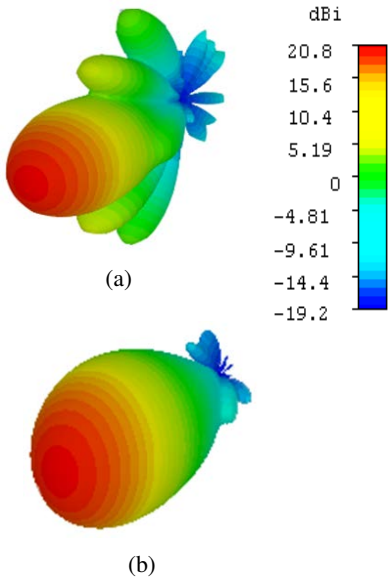

(a)

(b)

Fig. 5: 3D radiation pattern. (a) Metal-based horn antenna, (b) Graphene-based horn antenna.

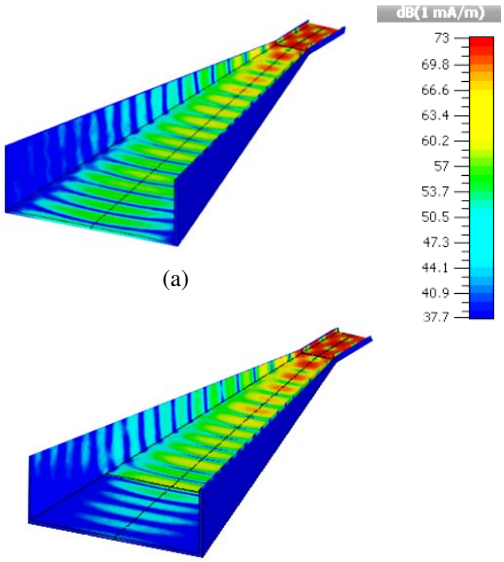

(a)

(b)

Fig. 6: Amplitude of the surface currents on the antenna lower wall. (a) Metal-based horn, (b) Graphene-based horn.

tible reduction in its amplitude, as shown in Fig. 6a. As a result, they trigger diffractions from aperture edges and unwanted radiations. According to Fig. 6b, graphene sheets can significantly suppress surface currents. As a result, by adjusting graphene surface impedance surface currents will be diminished correspondingly.

To wrap it up, results expressed a substantial improvement in SLL of the proposed horn antenna (Graphene-based horn) compared with the traditional one (Metal-based horn), as summarized in Table. I. Numerically calculated results illustrate that return loss of the suggested structure (Graphene-based horn) has remained under $-25dB$ in a broad frequency band. Therefore, graphene sheets did not cause any impedance mismatch in suggested antenna. However, the beam-width of the Graphene-based horn increased due to gain reduction and the tapered distribution of the aperture electric field.

TABLE I: Radiation Characteristics of the Proposed Antenna Is Compared with Traditional Horn Antenna.

Antenna Type	**Antenna far-field specification**			
	SLL (dB)	*F/B (dB)*	*Gain (dB)*	*Beam-Width (degree)*
Metal-based horn	-13.4	37	20.9	16.6
Graphene-based horn	-31	40	18.5	21

IV. Conclusion

We have presented a novel graphene-based method to reduce and control the side-lobe level of the traditional pyramidal horn antenna at microwave frequencies. Graphene length and surface impedance have been optimized in order to achieve a low side-lobe level of $-31dB$. The advantage of the proposed method over previously developed methods is its simple fabrication, and also its ability to achieve a desired side lobe level by adjusting the surface impedance of graphene through external biasing voltage.

References

[1] A. K. Geim, "Graphene: status and prospects," *science*, vol. 324, no. 5934, pp. 1530–1534, 2009.

[2] A. K. Geim and K. S. Novoselov, "The rise of graphene," *Nature materials*, vol. 6, no. 3, pp. 183–191, 2007.

[3] K. S. Novoselov, A. K. Geim, S. Morozov, D. Jiang, Y. Zhang, S. Dubonos, , I. Grigorieva, and A. Firsov, "Electric field effect in atomically thin carbon films," *science*, vol. 306, no. 5696, pp. 666–669, 2004.

[4] D. L. Sounas and C. Caloz, "Gyrotropy and nonreciprocity of graphene for microwave applications," *Microwave Theory and Techniques, IEEE Transactions on*, vol. 60, no. 4, pp. 901–914, 2012.

[5] S. Bae, H. Kim, Y. Lee, X. Xu, J.-S. Park, Y. Zheng, J. Balakrishnan, T. Lei, H. R. Kim, Y. I. Song *et al.*, "Roll-to-roll production of 30-inch graphene films for transparent electrodes," *Nature nanotechnology*, vol. 5, no. 8, pp. 574–578, 2010.

[6] X. Li, W. Cai, J. An, S. Kim, J. Nah, D. Yang, R. Piner, A. Velamakanni, I. Jung, E. Tutuc *et al.*, "Large-area synthesis of high-quality and uniform graphene films on copper foils," *Science*, vol. 324, no. 5932, pp. 1312–1314, 2009.

[7] H. Skulason, H. Nguyen, A. Guermoune, V. Sridharan, M. Siaj, C. Caloz, and T. Szkopek, "110 ghz measurement of large-area graphene integrated in low-loss microwave structures," *Applied Physics Letters*, vol. 99, no. 15, p. 153504, 2011.

[8] Y. Wu, Y. Xu, Z. Wang, C. Xu, Z. Tang, Y. Chen, and R. Xu, "Microwave transmission properties of chemical vapor deposition graphene," *Applied Physics Letters*, vol. 101, no. 5, p. 053110, 2012.

[9] J.-U. Park, S. Nam, M.-S. Lee, and C. M. Lieber, "Synthesis of monolithic graphene–graphite integrated electronics," *Nature materials*, vol. 11, no. 2, pp. 120–125, 2012.

[10] D.-Y. Jeon, K. J. Lee, M. Kim, D. C. Kim, H.-J. Chung, Y.-S. Woo, and S. Seo, "Radio-frequency electrical characteristics of single layer

graphene," *Japanese Journal of Applied Physics*, vol. 48, no. 9R, p. 091601, 2009.

[11] R. Murali, Y. Yang, K. Brenner, T. Beck, and J. D. Meindl, "Breakdown current density of graphene nanoribbons," *Applied Physics Letters*, vol. 94, no. 24, p. 243114, 2009.

[12] A. Tomaz, J. J. Barroso, and U. C. Hasar, "Side lobe reduction in an x-band horn antenna loaded by a wire medium," *Journal of Aerospace Technology and Management*, vol. 7, no. 3, pp. 307–313, 2015.

[13] M. Wang, C. Huang, M. Pu, and X. Luo, "Reducing side lobe level of antenna using frequency selective surface superstrate," *Microwave and Optical Technology Letters*, vol. 57, no. 8, pp. 1971–1975, 2015.

[14] C. A. Balanis, *Antenna theory: analysis and design*. John Wiley & Sons, 2005, vol. 1.

[15] J. Teniente, R. Gonzalo, and C. D. Río, "Low sidelobe corrugated horn antennas for radio telescopes to maximize," *Antennas and Propagation, IEEE Transactions on*, vol. 59, no. 6, pp. 1886–1893, 2011.

[16] C. Granet and G. L. James, "Design of corrugated horns: a primer," *Antennas and Propagation Magazine, IEEE*, vol. 47, no. 2, pp. 76–84, 2005.

[17] R. Elliott, "On the theory of corrugated plane surfaces," *Antennas and Propagation, Transactions of the IRE Professional Group on*, vol. 2, no. 2, pp. 71–81, 1954.

[18] C. Mentzer, L. Peters Jr *et al.*, "Pattern analysis of corrugated horn antennas," *Antennas and Propagation, IEEE Transactions on*, vol. 24, no. 3, pp. 304–309, 1976.

[19] B. M. Thomas and K. J. Greene, "A curved-aperture corrugated horn having very low cross-polar performance," *Antennas and Propagation, IEEE Transactions on*, vol. 30, no. 6, pp. 1068–1072, 1982.

[20] H.-S. Tae, K.-S. Oh, S.-E. Hong, M.-S. Lee, and J.-W. Yu, "Low side-lobe horn antenna with nonuniform slot array," *Microwave and Optical Technology Letters*, vol. 56, no. 8, pp. 1860–1862, 2014.

[21] W. D. Burnside and C. Chuang, "An aperture-matched horn design," *Antennas and Propagation, IEEE Transactions on*, vol. 30, no. 4, pp. 790–796, 1982.

[22] M. Aldrigo, M. Dragoman, A. Costanzo, and D. Dragoman, "Graphene as a high impedance surface for ultra-wideband electromagnetic waves," *Journal of Applied Physics*, vol. 114, no. 18, p. 184308, 2013.

[23] V. Gusynin, S. Sharapov, and J. Carbotte, "Magneto-optical conductivity in graphene," *Journal of Physics: Condensed Matter*, vol. 19, no. 2, p. 026222, 2007.

[24] G. W. Hanson, "Dyadic green's functions for an anisotropic, non-local model of biased graphene," *Antennas and Propagation, IEEE Transactions on*, vol. 56, no. 3, pp. 747–757, 2008.

[25] C. Xu, Y. Jin, L. Yang, J. Yang, and X. Jiang, "Characteristics of electro-refractive modulating based on graphene-oxide-silicon waveguide," *Optics express*, vol. 20, no. 20, pp. 22 398–22 405, 2012.

[26] M. Liu, X. Yin, E. Ulin-Avila, B. Geng, T. Zentgraf, L. Ju, F. Wang, and X. Zhang, "A graphene-based broadband optical modulator," *Nature*, vol. 474, no. 7349, pp. 64–67, 2011.